

## SPICE EUV spectrometer for the Solar Orbiter mission

A. Fludra<sup>a</sup>, D. Griffin<sup>a</sup>, M. Caldwell<sup>a</sup>, P. Eccleston<sup>a</sup>, J. Cornaby<sup>a</sup>, D. Drummond<sup>a</sup>, W. Grainger<sup>a</sup>, P. Greenway<sup>a</sup>, T. Grundy<sup>a</sup>, C. Howe<sup>a</sup>, C. McQuirk<sup>a</sup>, K. Middleton<sup>a</sup>, O. Poyntz-Wright<sup>a</sup>, A. Richards<sup>a</sup>, K. Rogers<sup>a</sup>, C. Sawyer<sup>a</sup>, B. Shaughnessy<sup>a</sup>, S. Sidher<sup>a</sup>, I. Tosh<sup>a</sup>, S. Beardsley<sup>a</sup>, G. Burton<sup>a</sup>, A. Marshall<sup>a</sup>, N. Waltham<sup>a</sup>, S. Woodward<sup>a</sup>, T. Appourchaux<sup>b</sup>, A. Philippon<sup>b</sup>, F. Auchere<sup>b</sup>, E. Buchlin<sup>b</sup>, A. Gabriel<sup>b</sup>, J.-C. Vial<sup>b</sup>, U. Schühle<sup>c</sup>, W. Curdt<sup>c</sup>, D. Innes<sup>c</sup>, S. Meining<sup>c</sup>, H. Peter<sup>c</sup>, S. Solanki<sup>c</sup>, L. Teriaca<sup>c</sup>, M. Gyo<sup>d</sup>, V. Büchel<sup>d</sup>, M. Haberleiter<sup>d</sup>, D. Pfiffner<sup>d</sup>, W. Schmutz<sup>d</sup>, M. Carlsson<sup>e</sup>, S.V. Haugan<sup>e</sup>, J. Davila<sup>f</sup>, P. Jordan<sup>f</sup>, W. Thompson<sup>f</sup>, D. Hassler<sup>g</sup>, B. Walls<sup>g</sup>, C. Deforest<sup>g</sup>, J. Hanley<sup>g</sup>, J. Johnson<sup>g</sup>, P. Phelan<sup>g</sup>, L. Blecha<sup>h</sup>, H. Cottard<sup>h</sup>, G. Paciotti<sup>h</sup>, N. Autissier<sup>j</sup>, Y. Allemand<sup>j</sup>, K. Relecom<sup>j</sup>, G. Munro<sup>k</sup>, A. Butler<sup>k</sup>, R. Klein<sup>m</sup>, A. Gottwald<sup>m</sup>

<sup>a</sup>RAL Space, STFC Rutherford Appleton Laboratory, UK; <sup>b</sup>Institut d'Astrophysique Spatiale, Centre universitaire d'Orsay, France; <sup>c</sup>Max-Planck-Institut für Sonnensystemforschung, Germany; <sup>d</sup>Physikalisch-Meteorologisches Observatorium Davos and World Radiation Centre, Switzerland; <sup>e</sup>Institute of Theoretical Astrophysics, University of Oslo, Norway; <sup>f</sup>NASA Goddard Space Flight Center, USA; <sup>g</sup>Southwest Research Institute, USA; <sup>h</sup>Almatech, Lausanne, Switzerland; <sup>j</sup>APCO Technologies, Switzerland; <sup>k</sup>European Space Tribology Laboratory, ESR Technology, UK; <sup>m</sup>Physikalisch-Technische Bundesanstalt, Germany

### ABSTRACT

SPICE is a high resolution imaging spectrometer operating at extreme ultraviolet wavelengths, 70.4 – 79.0 nm and 97.3 - 104.9 nm. It is a facility instrument on the Solar Orbiter mission. SPICE will address the key science goals of Solar Orbiter by providing the quantitative knowledge of the physical state and composition of the plasmas in the solar atmosphere, in particular investigating the source regions of outflows and ejection processes which link the solar surface and corona to the heliosphere. By observing the intensities of selected spectral lines and line profiles, SPICE will derive temperature, density, flow and composition information for the plasmas in the temperature range from 10,000 K to 10MK. The instrument optics consists of a single-mirror telescope (off-axis paraboloid operating at near-normal incidence), feeding an imaging spectrometer. The spectrometer is also using just one optical element, a Toroidal Variable Line Space grating, which images the entrance slit from the telescope focal plane onto a pair of detector arrays, with a magnification of approximately x5. Each detector consists of a photocathode coated microchannel plate image intensifier, coupled to active-pixel-sensor (APS). Particular features of the instrument needed due to proximity to the Sun include: use of dichroic coating on the mirror to transmit and reject the majority of the solar spectrum, particle-deflector to protect the optics from the solar wind, and use of data compression due to telemetry limitations.

**Keywords:** Solar instrumentation, EUV spectroscopy, VUV spectroscopy, spectrometer, spectrograph, imaging spectrometer, solar spectra, Solar Orbiter

## 1. INTRODUCTION

### 1.1 Solar Orbiter

Solar Orbiter is a mission of collaboration between ESA and NASA, selected as the first medium (M)-class mission of ESA's Cosmic Vision 2015 – 2025 programme for launch in 2017. Solar Orbiter's goal is to address the central question of Heliophysics: how does the Sun create and control the heliosphere? Solar Orbiter ([1], [2]) is specifically designed to identify the origins and causes of the solar wind, the heliospheric magnetic field, the solar energetic particles, the transient interplanetary disturbances, and the Sun's magnetic field itself.

It has been long known that many physical processes crucial in the formation and activity of the heliosphere take place much closer to the Sun than 1 AU, and that by the time magnetic structures, shocks, energetic particles and solar wind pass by Earth they have already evolved and in many cases mixed so as to blur the signatures of their origin. It is clear that flying a spacecraft with a combined remote-sensing and in-situ payload into the inner solar system will critically advance our knowledge.

Common to all mission science objectives is the requirement that Solar Orbiter make in-situ measurements of the solar wind plasma, fields, waves, and energetic particles close enough to the Sun, so that they are still relatively pristine and have not had their properties modified by dynamical evolution during their propagation. Solar Orbiter must also relate these in-situ measurements back to their source regions and structures on the Sun through simultaneous, high-resolution imaging and spectroscopic observations both in and out of the ecliptic plane. The only instrument onboard Solar Orbiter capable of spectroscopic on-disk observations is the SPICE spectrometer (Spectral Investigation of the Coronal Environment) which is described in this paper.

## 1.2 SPICE science objectives

SPICE is a high resolution imaging spectrometer operating at extreme ultraviolet wavelengths. It will address the key science goals of the Solar Orbiter mission, by providing the quantitative knowledge of the physical state and composition of the plasmas in the solar atmosphere, in particular investigating the source regions of outflows and ejection processes which link the solar surface and corona to the heliosphere.

SPICE is designed to study the structure, dynamics and composition of the corona by observing key emission lines on the solar disk on timescales from seconds to tens of minutes. A key aspect of the SPICE observing capability is the ability to quantify the spatial and temporal signatures of temperature and density tracers to unravel the inter-relationship between the chromosphere, coronal structures, coronal mass ejections, the solar wind, and the low corona.

The two EUV wavelength bands, 70.4 – 79.0 nm and 97.3 – 104.9 nm, observed by SPICE are dominated by emission lines from a wide range of ionized atoms of H, C, O, N, Ne, S, Mg, Si, and Fe, formed in the Sun’s atmosphere at temperatures from 10 thousand to 10 million Kelvin. A selection of representative lines over the entire temperature range is given in Table 1, including the First Ionization Potential (FIP) of each element and the mass-to-charge ratio (M/q) of the corresponding ions. The two SPICE passbands provide:

- Complete temperature coverage from the low chromosphere to the flaring corona,
- A range of strong coronal (Li-like) resonance lines,
- Detailed composition diagnostic capability of high and low FIP ion species as well as ions with different mass to charge (M/q) ratios to be compared with in-situ composition measurements on Solar Orbiter.

Table 1. SPICE line list

Ion	Wavelength (Å)	Log T (K)	FIP (eV)	M/q
H I Ly $\beta$	1025	4.0	13.6	---
C II	1036	4.3	11.3	12.0
C III	977	4.5	11.3	6.0
O IV	787.7	5.2	13.6	5.3
O V	760	5.4	13.6	4.0
O VI	1032	5.5	13.6	3.2
O VI	1037	5.5	13.6	3.2
S V	786.5	5.2	10.36	8.0
Ne VI	1005	5.5	21.6	4.0
Ne VII	973	5.6	21.6	3.3

Ne VIII	770	5.8	21.6	2.8
Mg VIII	772	5.9	7.7	3.4
Mg IX	706	6.0	7.7	3.0
Mg XI	997	6.2	7.7	2.4
Si VII	1049	5.6	8.1	4.8
Si XII	521 (2 <sup>nd</sup> )	6.5	8.1	2.6
Fe X	1028	6.0	7.9	6.2
Fe XVIII	975	6.9	7.9	3.3
Fe XX	721	7.0	7.9	2.9

Auxiliary lines:

Ne VIII	780	5.8	21.6	2.8
Si XII	499 (2 <sup>nd</sup> )	6.5	8.1	2.6

SPICE will measure plasma temperature, ‘emission measure’  $EM = \int Ne^2 dV$ , flow velocities, the presence of plasma turbulence, plasma composition and the dependence of elemental abundances of the solar plasma on the First Ionization Potential. It will be observing, at all latitudes, the energetics, dynamics and fine-scale structure of the Sun’s magnetized atmosphere.

Study of shape and position of emission lines will yield plasma velocity along the line of sight and line broadening parameters. Study of emission line strengths will yield temperatures, emission measure, densities, and elemental abundances. Two primary modes of observation will therefore be: (a) dynamics studies, involving rapid on-disk scans over smaller areas a few arcminutes wide and recording profiles of a small number of bright lines (shaded rows in Table 1), and (b) slower composition scans using longer exposure times, covering large areas up to 16 arcmin wide and recording intensities of lines from all elements. SPICE will provide maps of outflow velocities, and mass-to-charge ratio of surface composition features, connecting them to solar wind structures observed by in-situ instruments. SPICE will carry out the first-ever out-of-ecliptic spectral observations of the solar polar regions.

Spatially resolved UV imaging spectroscopy is an essential tool to study Sun’s atmosphere. SPICE is the only instrument onboard Solar Orbiter providing the plasma diagnostic capability for these studies. It will remotely determine plasma properties on the Sun and provide understanding of the linkage between in-situ measurements of solar wind streams using the suite of plasma instruments on Solar Orbiter and remote imaging of their source regions on and near the Sun. Detailed SPICE science goals, required observations and measurement objectives relating to four top-level science objectives of Solar Orbiter [2] are given in Table 2.

SPICE is intended to operate as part of a suite of instruments onboard Solar Orbiter and in coordination with Solar Probe and near-earth spacecraft, providing a unique opportunity for correlative measurements. SPICE will be capable of collecting data on a nearly continuous basis and executing campaign observations that are planned jointly with the other instrument teams onboard Solar Orbiter and other appropriate near-earth and deep-space instruments.

Table 2. SPICE science goals and measurements

Science Question	Required SPICE Observations	SPICE Measurement Objective
2.1.1 What are source regions of the solar wind & heliospheric magnetic field?	Composition of solar wind source regions	Determine FIP and Q/M effect in solar wind source regions
	Spectral images of chromosphere & corona	Identify feature types that give rise to the solar wind by correlating Doppler shift to structure and composition
2.1.2 What mechanisms heat and accelerate the solar wind?	High-res spectral images of loops & evolving structures	Evolution of source regions on time scale of network evolution. Measure outflow (from Doppler shift) and correlate with structure type.
	Wave propagation and heating	Line width, Doppler shift, & Intensity time series observations
	Off-limb observations of non-thermal velocities	Off-limb line profile measurements in H Ly- $\beta$ , Ne VIII & O VI up to 1.15Rs @0.3 AU
2.1.3 What are the sources of solar wind turbulence and how does it evolve?	Images of source regions in Doppler-broadened lines	Identify jets, heating, and turbulence; correlate to network evolution
2.2.1 How do CMEs evolve through the corona and inner heliosphere?	Map CME source location, expansion, rotation and composition	Identify areas of coronal dimming; Measure velocities in the erupting CME; Establish identity of plasma in visible parts of a proto-CME on-disk and connect (via compositional correlation) to higher altitudes and in situ measurements
2.2.2 How do CMEs contribute to solar magnetic flux and helicity balance?	Map source regions to in-situ properties: magnetic connectivity, polarity, & helicity	Establish identity of plasma in visible parts of a proto-CME on-disk and connect (via compositional correlation) to higher altitudes and in situ measurements
	High-resolution coronal and chromospheric images	Establish identity of plasma in different parts of a proto-CME and connect (via compositional correlation) to higher altitudes and in situ measurements
2.3.1 How and where are energetic particles accelerated at the Sun?	UV & X-ray imaging of loops, jets, flares, and CMEs	Identify jets and reconnection sites that give rise to SEPs
2.3.2 How are energetic particles released from their sources and distributed in space and time?	Timing, location and intensity profiles of VUV emissions in relation to energetic particle intensities at a wide range of energies	Provide thermodynamic characteristics of plasmas in the SEP sources. Establish identity of plasma supplying SEPs and connect (via compositional correlation) to higher altitudes and in situ measurements

2.4.1 How is magnetic flux transported to and re-processed at high solar latitudes?	High-resolution images of small-scale magnetic features at the poles	Determine evolution of magnetized regions on the time scale of network evolution, by observing evolution of the structure seen in the EUV emission and associated flows. Reveal the pattern of differential rotation in the chromospheric and transition region emission.
2.4.2 What are the properties of the magnetic field at high solar latitudes?	Line-of-sight plasma flows, spatial distributions of intensities of chromospheric and transition region lines, and temperatures of polar regions	Identify feature types that give rise to the solar wind by correlating Doppler shift to structure and composition. Contribute to the investigation of the 3D structure of the inner heliosphere – study the links between the polar regions and the in-situ properties of the solar wind and the IMF.  Study the response in the EUV emission to the magnetic field cancellation process.

## 2. INSTRUMENT OVERVIEW

The SPICE instrument is an imaging spectrograph which records high resolution EUV spectra of the Sun. The SPICE optical design is based on the comprehensive work carried out during the earlier phases of the project. The instrument optics unit (SOU) mechanical design and layout are shown in Figure 1 and the optical path is shown in Figure 2.

As shown in Figure 1, the light enters the instrument through the entrance aperture, then an image is formed at the slit by the off-axis parabola mirror. The slit defines the portion of the solar image that is allowed to pass onto a concave Toroidal Variable Line Space (TVLS) grating, which disperses, magnifies, and re-images incident radiation onto two detectors. The two wavebands cover the same one-dimensional spatial field, and are recorded simultaneously. Details of the optical path are further described in Section 3.

The instrument contains four mechanisms:

- The SPICE Door Mechanism (SDM) which can be actuated to provide a contamination tight seal of the entrance aperture during non-operational periods (both during ground handling and non-operational periods in flight).
- The telescope mirror is mounted to a two-axis mechanism (tilt and focus), the scan focus mechanism (SFM), that is used to direct different portions of the solar image onto the selected entrance slit and to focus the telescope relative to the entrance slit. The image of the Sun is repeatedly scanned across the entrance slit. During each scan the image of the Sun is stepped across the entrance slit in increments equal to the selected slit width, such that the region of interest is completely sampled.
- A slit change mechanism (SCM) provides four interchangeable slits of different widths, one of which can be selected depending upon the science activities to be conducted. In the nominal design these slits have a 2", 4", 6" and 30" width on the external field of view.
- A vacuum door mechanism on the Detector Assembly. The micro-channel plate and image intensifier used to translate the incident EUV photons into visible light photons which can be detected by the detectors must be maintained either at vacuum or in zero humidity during ground handling. Therefore the detector assembly contains a door mechanism which is only opened during vacuum testing on ground, and opened finally once on-orbit.

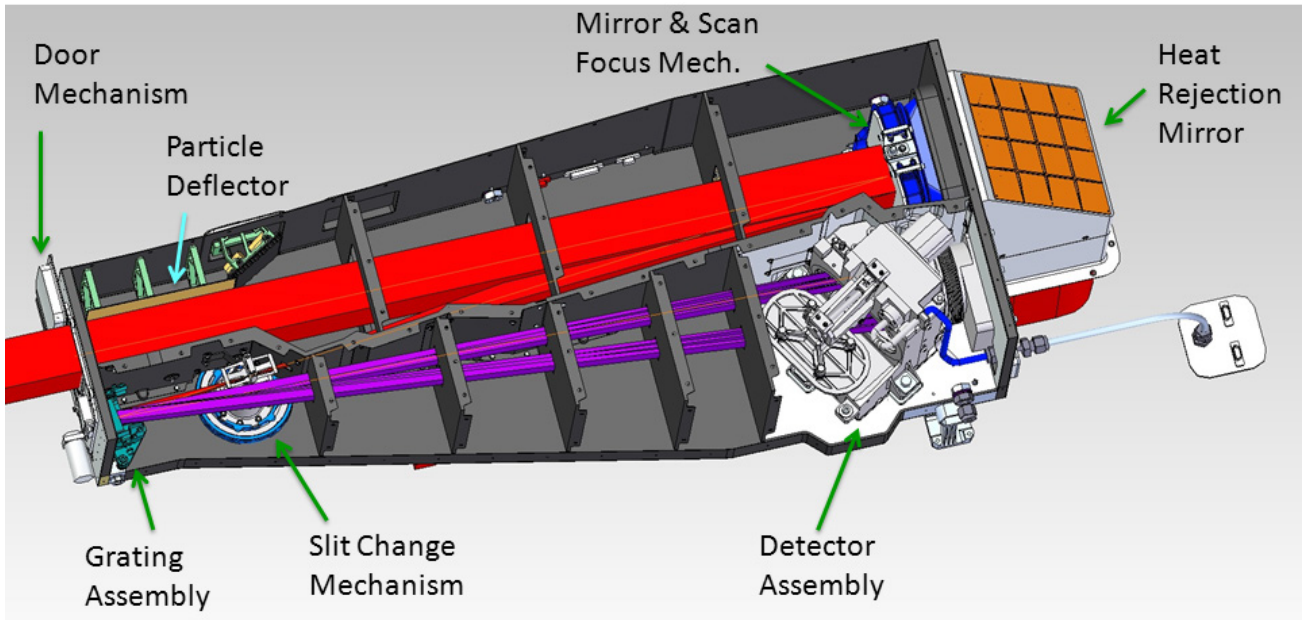


Figure 1. SPICE Optics Unit with major subsystems identified.

The instrument structure consists of a Carbon Fibre Reinforced Plastic and Aluminium honeycomb baseplate with side walls and lids also made from Carbon Fibre panels. This is isostatically mounted to the spacecraft panel. The structure is designed to have approximately zero CTE, therefore maintaining instrument alignment throughout the wide operating temperature range.

The instrument control function will be provided by a dedicated electronics box, the SPICE Electronics Box (SEB). This provides the drive and monitoring for all mechanisms, the acquisition and processing of all housekeeping telemetry and the processing and packetisation of the science data. It controls and communicates with the detector front end electronics (FEE) via a SpaceWire link. The SEB also contains the SPICE flight software (FSW) which is responsible for all control and monitoring of the instrument, plus the processing and compression of the science data to allow the data rate and volume requirements to be achieved.

### 3. OPTICAL LAYOUT

The optical system is shown in Figure 2, and the key optical parameters are listed in Table 1.

The light enters the instrument through the entrance aperture (defined by the frame of the SPICE Door Mechanism), then an image is formed at the slit by the off-axis parabola mirror. The mirror off-axis distance corresponds to an off-axis angle of the principal ray of 5 degrees. The mirror substrate is synthetic fused silica Suprasil 300. The mirror coating is a thin layer of boron carbide (B4C) of 10 nm thickness, chosen to optimize the trade-off in its dichroic property, i.e., between wanted maximum reflection in the EUV science wavelengths, and minimum reflection or absorption of the solar visible and near infrared. In this way the mirror achieves reflectivity of ~30% in the EUV while allowing the majority, i.e., ~90% of the solar energy to pass through the primary mirror and ultimately back out to deep space via the heat rejection mirror and SPICE exit aperture. Although the part of the mirror used for the EUV imaging is only the central ~50 mm x 50 mm, the mirror size has to be ~10 cm x 10 cm square, in order to accommodate this solar heat transmission heat-dump scheme, for all SPICE pointing positions on the solar disc.

The primary mirror is mounted on a Scan-Focus mechanism which allows:

- 1) The re-focus of the telescope, needed under the variable high solar heat loads
- 2) the rastering of the slit image on the sky. This scanning is done by rotation of the mirror about the centre of the front face of the mirror, and over the raster-FOV angular range it has small impact on the imaging aberrations.

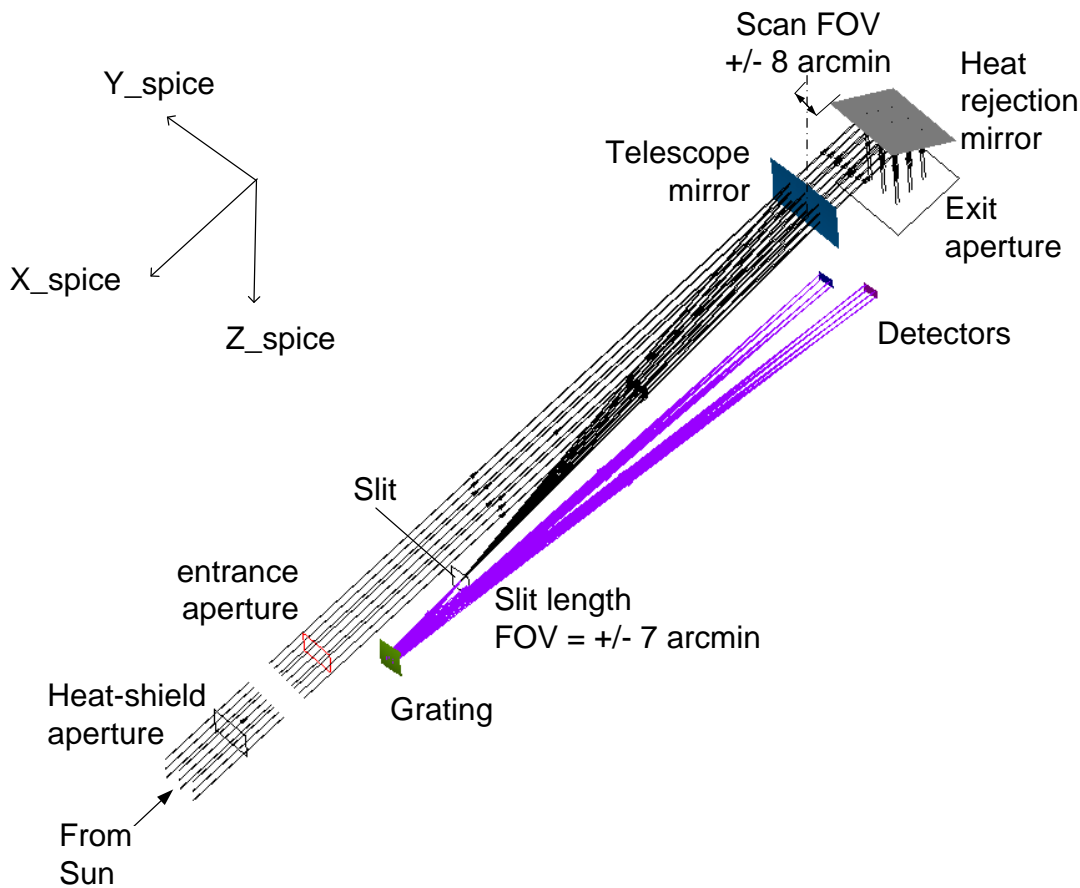


Figure 2. SPICE optical layout.

Although the mirror only reflects a small portion of the solar energy, it is necessary to prevent this from entering the spectrometer, and so there is a pre-slit mirror, placed ahead of the mirror focal plane. This is a plane mirror which surrounds the used optical beam, and it has a central slit aperture, such that it reflects the imaged solar disc out of the optical path, except for the wanted instantaneous-FOV.

The slit defines the portion of the solar image that is input to the spectrometer, thus the slit-length defines the instantaneous-FOV. There are 4 interchangeable slits. The design is such that the aberration blur-diameter of the telescope imaging is approximately equal to the width of the narrowest slit (i.e.  $6\mu\text{m}$ ), at the worst case FOV positions.

The spectrometer section uses a single optical element, a reflective grating, in order to maximize optical throughput (reflectivity is  $\sim 30\%$  per surface at near-normal incidence between  $40\text{ nm}$  and  $200\text{ nm}$ ). The grating design is a concave Toroidal Variable Line Space (TVLS) type. It disperses, magnifies, and re-images the SPICE slit onto two detector arrays, covering the two separate science bands, with wavelength ranges as shown in Table 1. The imaging magnification is approximately  $\times 5$ , leading to the large grating-to-detector distance, and this distance varies in the dispersion direction, because the image plane is oblique (i.e. not perpendicular to the beam). The required control of the aberrations to within  $\sim 1$  pixel is demanding in this single-element design for the SPICE spatial and spectral ranges, in particular the control of astigmatism. This type of design is made possible by the use of the toroidal surface form and the matching varied line space or ‘chirped’ ruling, of the type developed originally for spherical substrates in Ref. [3], [4] and developed for solar instruments in Ref. [5]. For SPICE the toroidal form has sagittal radius =  $213.5\text{ mm}$ , tangential radius =  $214.9\text{ mm}$ , with this toricity precisely matched to the chirp.

Table 3. SPICE optical parameters

Parameter	Value/Description	Units
<i>Front baffle (SO heat-shield)</i>		
Feedthrough aperture size and location	50x50, distance 425 ahead of SPICE aperture	mm
<i>Telescope</i>		
Entrance aperture size and location	43.5x43.5, distance 771 ahead of telescope mirror	mm
Focal length of parent paraboloid	622	mm
off-axis-distance	55	mm
effective focal length of PM	623.21	mm
f-number	14.3	-
Plate scale at slit	3.02	µm/arcsec
Instantaneous FOV	slit length ('north-south'): 13 arcmin, plus 0.5 x0.5 arcmin 'dumbbell' image regions at each end	
Rastered FOV	Scan range ('east-west'): +/-8 arcmin, by rotation of primary mirror	arcmin
Angular range of heat-dump optics	+/- 1 solar-disc diameter at 0.28AU	-
<i>Slits</i>	widths = 2, 4, 6 and 30	arcsec
<i>Spectrometer</i>		
Wavelength range, SW	70.387 to 79.019 (1st order)	nm
Wavelength range, LW	97.254 to 104.925 (1st order) 48 to 53 (2nd order)	nm
slit to grating distance	128	mm
grating groove density and +/- chirp	2400 +/- 1.7%	grooves/mm
grating image distance, SW mid-band	692.43	mm
grating image distance,LW mid-band	720	mm
detector pixel spacing	0.018	mm
dispersion, at image plane	0.0095 at 74 nm 0.0083 at 101 nm	nm wavelength per pixel spacing
APS usable pixels	968 x2 bands spectral pixels, 800 spatial pixels	
<i>System focal length (SW)</i>	3.371	m
<i>System spatial plate scale</i>	1.101 at 74 nm 1.059 at 101 nm	arcsec per pixel

#### 4. DETECTOR ASSEMBLY

The SPICE detectors consist of two independent, identical, intensified APS camera systems mounted in a common sealed housing. Each camera consists of a HAS2 (High Accuracy Startracker 2) 1024 x 1024 format CMOS APS with digital readout electronics fed by a KBr coated MCP intensifier. The APS detectors are cooled to -20 °C during operation.

The SPICE intensifier tubes consist of a microchannel plate (MCP) and a phosphor screen packaged in a lightweight housing. Each will provide a nominally 25 mm diameter active area that circumscribes the sensor active area. A KBr photocathode is deposited on the front surface of the MCP to enhance response in the SPICE passbands, while remaining visible light blind. Photons absorbed by the KBr layer are converted to photoelectrons and amplified through the MCP based on the applied voltage across the MCP. Electrons exit the MCP pores and are accelerated by a further applied voltage, across a sealed proximity gap onto an aluminized phosphor screen deposited onto a fibre optic output window. The resulting cathodoluminescence image is transferred through a fibre optic coupler to the APS sensor. The detector Front End Electronics (FEE) that reads out the data from the two APS sensors is described in Section 6.1.

## 5. INSTRUMENT PERFORMANCE

The performance parameters described here are summarised in Table 4.

Table 4. SPICE instrument key performance parameters

Parameter	Predicted performance	Conditions/assumptions
<b>Spectral characteristics</b>		
LSF width (at 2" slit)	4 pixels FWHM	slit, spectrometer aberrations, detector PSF. Worst-case FOV
Spectral resolving power	2000 mid-band SW	Calculated as wavelength/FWHM
	3000 mid-band LW	
Out of band response	2nd-order 48-53 nm: 3% of LW response, 6% of SW	grating scatter, detector solar-blind
	Scatter < 1 detected-photon/second per pixel	
<b>Spatial characteristics</b>		
PSF width (along-slit)	4 pixels FWHM	system aberrations, detector PSF. Worst-case FOV
Out-of-field response due to the solar disk	Background level 0.01% of solar disk average radiance at 8 arcmin from limb	mirror: micro roughness 0.2 nm particulate cleanliness 300 ppm
<b>Sensitivity</b>		
Effective area	~5 mm <sup>2</sup> in SW ~10 mm <sup>2</sup> in LW	mirror, grating, detector efficiencies, @BOL
Range of signal rates (3 SPICE lines: O VI, Ne VIII, Mg IX) in active region	7000 photon/s (O VI) 100 photon/s (Ne VIII) 4 photon/s (Mg IX)	detected-photon levels
Instrument noise terms (1-sigma)	MCP amplification 1.5 x photon-noise	measured in detector tests
	dark current 0.5 photon/s per pixel	
	read-noise 3 photon/pixel	
Exposure times to reach line-SNR = 10 in active region	0.04 s (O VI) 3 s (Ne VIII) ~100 s (Mg IX)	Based on line intensities measured by SOHO/SUMER

## 5.1 Imaging resolution

In the spatial (i.e. along-slit) direction, the image quality (assessed in terms of point-spread-function PSF) is made up of several contributors with the following full-width-at-half-maxima (FWHM), at the worst-case FOV position: aberrations of the nominal design (2.5 pixels); aberrations due to as-built effects (components wave-front-error quality, and accuracy plus stability achieved in the alignment, increasing the FWHM to 3.5 pixels); and the PSF response of the detector system. For the latter the PSF width is larger than the pixel spacing, due to signal spatial spreading effects. It is characterised in terms of modulation-transfer-function (MTF) and when converted to equivalent PSF using gaussian response model it contributes a FWHM of 1.8 pixels. The net spatial PSF then has FWHM ~4 pixels.

In the spectral direction, for the spectral line-spread-function (LSF) the optical aberration contribution is different, as it involves only the spectrometer portion of the system, i.e., after the slit, but in this case there is the additional contribution of the finite slit width. For the minimum width slit (i.e., 2 arcsecs), and taking into account the aberration and detector terms as above, leads to an LSF with FWHM in terms of pixels which is also approximately 4 pixels, in the worst-case instantaneous-FOV position. At the spectral plate-scale of ~0.01 nm per pixel, this leads to LSF width of ~0.04 nm, and so spectral resolution R with values of R~2000 at 74 nm wavelength and R~3000 at 101 nm wavelength.

## 5.2 Radiometric sensitivity

This is due to the product of the responses of the components in the signal path. These are the mirror and grating reflectivities (each ~0.3), the grating diffraction relative efficiency (~0.3), the detector system quantum detection efficiency (QDE ~0.13 detected photons per incident photon in SW, 0.25 in LW), and the expected factor for darkening due to molecular contamination (~0.8). Together these lead to effective areas of ~5mm<sup>2</sup> in the SW and ~10mm<sup>2</sup> in LW, i.e., approx. 0.35% and 0.7% of the instrument physical aperture area.

As a result, the signal photon rates, in terms of detected photons per second, in a few representative SPICE spectral lines (C III, O VI, Ne VIII and Mg IX), vary over typical solar targets from 7000 photons/second for O VI in active regions, to 110 photon/s for Ne VIII, to values as low as 4 photons/second for Mg IX in active regions, for the 2 arcsec slit and a 2 arcsec binning of pixels spatially.

The detector system noise is dominated by an amplification of the photon Poisson noise, by a factor of ~1.5, which occurs in the MCP. This gives resulting required exposure times (for the SPICE data product figure-of-merit which is time to reach line-signal-to-noise ratio SNR of 10), varying from ~0.04 seconds to a few seconds for bright lines, and over 100 seconds for weak lines. At this line-SNR the centroiding accuracy (for plasma Doppler-velocity determination) is ~0.15 pixels at 1-sigma uncertainty, and at the SPICE spectral dispersion the velocity scale is ~40 km/s per pixel.

## 5.3 Stray light

Stray light in the instrument affects two performance aspects:

- 1) Out-of-band response. This is detector signal due to light incident on any pixel at wavelengths other than that expected from the spectrometer dispersion design. As well as the response in 2<sup>nd</sup> diffraction order, it occurs by incoherent light scattering taking place after the slit, i.e. in the spectrometer (at the grating and the baffles). This produces an increased signal background level and so impacts on the instrument sensitivity.
- 2) Out-of-field response. This occurs also by incoherent light scatter, in the telescope (mirror and baffles). All such scatter is effectively in-band as it takes place ahead of the slit. It is an important effect for viewing of the solar corona (SPICE will be able to view at up to 8 arcmin above the solar limb, when the spacecraft is pointed at the limb). In this case it affects the sensitivity for detection of spectral lines in the faint corona above the background of scattered light from the bright solar disc.

For the out-of-band performance, the important aspects are: the degree of grating surface scatter, affected by substrate roughness plus ruling quality; the efficiency with which the various spectrometer baffles can trap the unwanted diffraction orders and spectral lines (in particular the zero-order light and the Lyman-alpha line); and the degree of 'solar-blindness' which the detector design can achieve (i.e., to reduce sensitivity to the bright UV-visible part of the solar spectrum). These aspects all have to be controlled, but a critical factor is the high degree of solar-blindness that is achievable. This has to have a very strong suppression of wavelengths >150 nm, where the solar spectrum starts to become very bright. In the SPICE detector a QDE of less than 10<sup>-4</sup> is achieved for wavelengths >200 nm. With the

anticipated grating scatter levels, the expected out-of-band stray light signal is at a level below that of the solar spectrum continuum of previous instruments in this band, i.e., < 1 photon per second per pixel, and so having minimum impact.

For the out-of-field performance, in order to minimize scattered light the mirror is made with low surface micro-roughness, to the level of ~0.2 nm RMS, and the particulates cleanliness level is kept to Surface Cleanliness Level ~200 (per IEST-STD-CC1246D standard), corresponding to obscuration factor ~300 ppm. This gives an out-of-field scatter level from the solar disc, of  $\sim 10^{-4}$  at 8 arcmin (i.e., 0.25 solar radii) above the limb. The spectral lines of interest that can be observed above the limb (Mg IX, O VI, Ne VIII) still have at least ~1% brightness at this height (relative to the on-disc average). So for these observations the signal-to-background ratio will be 100:1, and so this level of out-of-field rejection is adequate to allow these observations.

#### **5.4 Contamination control**

As an extreme-UV solar instrument, SPICE is very sensitive to molecular contamination by hydro-carbon compounds, which has a known effect of degradation on space hardware. Even at the best optical surface cleanliness levels achievable in-flight, of a couple of molecular layers on each surface, the effect of polymerization of these by direct solar UV light is known to produce significant darkening at EUV wavelengths. Hence there is a factor included for this effect in the above sensitivity description. The budgetary figure for this molecular contamination in SPICE is 200 ng/cm<sup>2</sup> over life. This level, and that of the required particulates cleanliness, is only achievable using: a) selection of suitable materials, b) stringent cleaning and bake-out processes during parts preparation, c) careful sealing and continuous purging of the optics compartment during all assembly and test right up until launch, and d) careful operations in-flight, such as the use of de-contamination heaters and the use of the SPICE door for protection from out-gassing products of the Solar Orbiter instruments and spacecraft, especially in the early mission phase.

The contamination control is also important for the properties of key thermal surfaces, such as the reflective surfaces on the outside of the SPICE door, on the heat-rejection-mirror and on the pre-slit, to preserve the SPICE thermal performance. For the external surfaces the molecular and particulate contamination levels are higher than the above values of the internal optics, as there is less protection possible.

## **6. ELECTRONICS**

### **6.1 Detector Front End Electronics (FEE)**

The SPICE FEE is based around the performance and specification of the HAS2 detector. It is a CMOS Active Pixel Sensor with 1024 x 1024 pixels on an 18  $\mu$ m pitch. The FEE has two HAS2 detectors, one for short wavelength signals, the other for long wavelength signals.

The FEE has one dual-channel signal processing Analogue-to-Digital Converter required to sample and digitise the video signals from the two HAS2 detectors. The ADC runs at up to 6.25 Mpixels/s, and provides 14 bit digitisation. The digitised video data is serialised and transferred to the FPGA where it is multiplexed and then passed via the SpaceWire interface to the SEB. The video gain and video offset for each readout channel can be programmed independently.

The FPGA has two main functions, the first being Waveform Generator and sequencer, the other being SpaceWire Interface. It also contains control and signal steering logic. The ACTEL RTAX FPGA carries a programmable Waveform Generator and Sequencer (WGS) and the HAS2 clock driver circuitry. The WGS defines the camera's HAS2 and video signal processing electronics timing signals with a resolution of 20 ns.

The SpaceWire Interface provides the FEE's communications with the control and data acquisition interface. The communications interface is a SpaceWire adaptation of the IEEE1355 serial interface standard, featuring an LVDS-driven SpaceWire serial data link running at 100 Mbits/s.

The FEE houses one electronics card, although split into four parts (two of which are physically in parallel) connected by flexi cables. The FEE will allow multiple windowed readout. Destructive and non-destructive readout modes are supported by appropriate programming of the FEE's Waveform Generator and Sequencer. Image size, readout sequences and window parameters are defined by programming the Waveform Generator and Sequencer's internal Readout Table memory from the FEE's control and data acquisition interface. Exposures can be defined and timed externally to the

FEE, but alternatively an internal timing routine could be set up within the Waveform Generator and Sequencer if required.

## 6.2 SPICE Electronics Box (SEB)

The SEB is an integrated electronics assembly that provides complete control and data processing for the SPICE instrument. Key capabilities of the SEB include:

1. High Voltage Power Supply outputs for the intensifier and the solar wind deflector
2. Closed loop control of the telescope focus and scan mechanisms, detector door and SPICE instrument door
3. Open loop control of the telescope slit change mechanism
4. Closed loop instrument thermal management
5. Redundant SpaceWire command and telemetry interface to the Solar Orbiter Spacecraft
6. Advanced image processing and compression for spectral images received from the detector Front End Electronics (FEE) via a dedicated Spacewire link.
7. Instrument safety management
8. The SEB integrates a low voltage power supply.

The SEB provides SPICE image processing based on the concept of spectral windows. These windows are dedicated slices of the focal (i.e. Y by  $\lambda$ ) plane. The readout of the FEE by the SEB is handled on a window by window basis. A high performance, pipelined architecture is optimized for minimal power dissipation while still providing the ability to continuously receive and process images in real time. The pipelined architecture includes five stages: non-destructive pixel readout, selectable black level correction, selectable binning, selectable dumbbell extraction for alignment tracking, frame accumulation for Spectral Hybrid Compression (SHC). The SHC algorithm provides up to 20:1 compression ratio of spectral data required to fit with the Solar Orbiter telemetry rate allocated to SPICE.

## 7. MECHANICAL DESIGN

### 7.1 Entrance Aperture and Heat Shield Feedthrough

A 52 x 52 mm square (with 2.5 mm radii corners) opening in the spacecraft heat-shield serves as the entrance aperture. Behind the heat shield aperture are three additional, equally spaced optical baffles. The SPICE entrance aperture is 29 mm behind the front of the SPICE Optical Unit (SOU) volume. This is a 43.2 x 43.2 mm rectangular opening defined by the mounting plate of the SPICE Door Mechanism (SDM). This defines the optical entrance aperture for the instrument. At perihelion, approximately 32 W of solar load enters the instrument through this aperture.

The heat shield aperture is oversized with respect to the instrument aperture to account for relative (thermo-elastic) movement between them and thus ensure a clear view from the instrument. This means that a region of the SDM mounting plate will be illuminated. The incident solar load on this region is approximately 8 W at perihelion.

### 7.2 SPICE Door Mechanism (SDM)

The SPICE door mechanism (SDM) includes a sliding door, positioned at the front of the SOU, which provides an open and closed aperture for the instrument. The SDM comprises a mounting plate to which a door paddle and drive mechanism is attached. A stepper motor moves the door paddle over the instrument knife-edge aperture. The door is closed to prevent contamination entering the instrument during on-ground test activities and on-orbit manoeuvres. The door will open/close to match the instrument observational windows.

Thermally, the door is designed to withstand the perihelion solar environment at end of life (EOL) should it remain closed and the heatshield door remain open. The +X facing surface of the door panel (that faces the door) is a concave mirror with a focal length of 700 mm designed to reflect the incoming solar beam back to space, without intercepting the spacecraft feedthrough. Thus the requirement on minimising solar load reflected to the feedthrough is achieved.

The front surface of the door and the aperture edge have a vacuum deposited silver coating to minimise the absorption of solar radiation when the door is closed (At BOL  $\alpha_s = 0.06$ ;  $\epsilon = 0.03$  and at EOL  $\alpha_s = 0.077$ ;  $\epsilon = 0.034$ ). The edges and rear of the door paddle are black coated. This selection of coating minimises the door temperature and the gradients across the linear bearings guiding the door paddle during movements. No specific thermal coatings are presently envisaged on other surfaces of the mechanism.

The door is thermally decoupled from the mechanism baseplate by virtue of the linear bearings and lead screw arrangement. The goal was to provide thermal control of the door without the need of a (flexible) thermal link to the hot element interface. The selection of the above thermo-optical finishes results in a peak (door closed) temperature of approximately 150 °C.

### **7.3 Scan Focus Mechanism**

The Scan Focus Mechanism (SFM) architecture comprises a flexure based stage supported on stiff flexural foot supports to maintain the location of the primary mirror relative to the underlying optical bench. Motion in both the scan (rotation about z) and focus (linear displacement in x) are possible due to the compliance of the structure in both of these degrees of freedom, while the stiffness is high in the others. The linear focus stage is the primary stage, allowing  $\pm 0.5\text{mm}$  of linear focus adjustment. The rotational scan stage is the secondary stage, mounted on the moving focus stage, and provides the rotational motion of the mirror over a range of 0 to 8 arc-minutes (corresponding to 16 arc-minutes total scan range).

The focus mechanism employs a roller screw to position the stage over the required  $\pm 0.5\text{mm}$  range. This is driven by a Phytion VSS space stepper motor via a 49:1 epicyclic (planetary) gearbox. The scan mechanism uses a CEDRAT PPA80L pre-stressed piezo-electric actuator to drive the torsionally compliant mirror support flexure via a lever arm arrangement.

Both stages have linear variable differential transducer (LVDT) position sensors, although only the scan stage has closed loop position control. The windings of each sensor are located on the moving focus stage with the core moving within. The focus sensor is connected directly to the static structure to sense the relative motion, while the scan sensor is connected to a lever arm on the rotational stage. This lever arm is designed to amplify the displacement such that a suitably accurate LVDT can be used. This ensures that the high resolution required for the scanning function can be achieved.

### **7.4 Slit Change Mechanism (SCM)**

The slit change mechanism is responsible for positioning any one of the four slits into the active slit position within the required absolute and repeatable tolerances. The assembly has a mechanical interface with the top face of the instrument optical bench and is supported by a titanium flange. A cut-out in the CFRP optical bench accommodates the rotary stepper motor (SAGEM #21 PP 61-04-03-WW) that sits at the base of the assembly. The stepper motor drives a Rollvis satellite screw which translates the rotary output of the stepper motor in to linear motion. Lubrication of the moving parts will be achieved through the use of either dry or hybrid lubricant that is hermetically sealed from the internal cavity of the optics unit.

The linear drive from the satellite screw moves the slit plate assembly in the Z direction to position the selected slit in place. The slit plate is guided by a pair of titanium leaf springs supported from the main structure. The SCM will incorporate mu-metal magnetic shielding that will greatly reduce the magnetic signature of the Sagem stepper motor to satisfy spacecraft magnetic cleanliness requirements.

Each of the four slits will be etched using precision lithography into a common piece of silicon wafer. The slits are then separately cut from this wafer and trimmed to the desired dimensions. Slit widths are 6  $\mu\text{m}$ , 12  $\mu\text{m}$ , 18  $\mu\text{m}$  and 90  $\mu\text{m}$ , corresponding to angular width of 2, 4, 6, and 30 arcsec. The slits are baselined to be the equivalent of 13 arcmin long, plus a 30 x 30 arcsec “dumbbell” at either end which is used during on-ground data processing to reconstruct the scanned images. The slits will be arranged within the slit holder in the following order: 6 arcsec slit, 2 arcsec slit, 4 arcsec slit, 30 arcsec slit. The most used slit (based on the operational planning), the 2 arcsec slit, is in the neutral position of the titanium leaf springs and is in place at launch.

### **7.5 Particle Deflector**

The thin boron carbide coating of the primary mirror is sensitive to damage from the solar wind protons at fluences greater than

The Particle Deflector consists of two plates of CFRP, of dimension 140 by 80 mm (by 1 mm thick), coated with a 0.5 micron thick layer of gold (on a layer of titanium as an adhesion promoter). Although the CFRP is reportedly conductive, the gold layer ensures good conductivity and gives a good surface onto which wires can be attached. One plate is held off from the outer sidewall with GFRP supports and the other is attached to the mid-wall of the structure, and is held 5 mm outside the expected thermal beam envelope. The plates are held more than 5 mm away from any grounded surface. At the foreseen voltage of 2.5 kV, examination of the Paschen curves shows that much smaller gaps could be tolerated. The separation of the plates is then 53 mm. The resultant electric field then deflects the incoming solar wind protons so they do not impact onto the primary mirror. The negative voltage plate is held 5mm away from any possible ground plane (lid or front panel).

Whilst the instrument door is open, voltage is applied to the plate. The plate held off from the outer sidewall is held at -2500 V, the other one at 0 V (referenced to instrument ground). Electrostatic finite element simulations have been performed and show that 1200 km/s protons do not impact the mirror in this configuration. The “mid-wall” plate is charged to negative voltage so that C-section baffle/support structure performs a secondary function as a proton trap. It is expected that the CFRP will scatter, via Rutherford scattering, the incoming protons. Therefore, traps are required.

## 8. THERMAL SYSTEM OVERVIEW

Solar Orbiter is targeted for an elliptical orbit about the Sun, with a minimum perihelion of 0.28 AU. The primary thermal challenge is managing the extreme ( $\sim 17 \text{ kW/m}^2$ ) heat input at perihelion. The thermal control system must also be compliant during periods with little or no solar loading and with the conditions during the Earth and Venus gravity assist manoeuvres required for orbit adjustment.

The nominal science mission covers about 3½ years and begins after the second Venus gravity assist manoeuvre. The primary operational periods for remote sensing instruments (‘encounters’) consist of a 10-day window centred on the perihelion and two 10-day windows centred around the highest latitudinal extents reached during each orbit. The total number of encounters is eight in the nominal mission and eight in the extended mission.

SPICE is accommodated behind the heatshield within the spacecraft. A feedthrough in the heatshield provides a view for the SPICE Optics Unit. The SOU is, with the exception of two designated heat rejection interfaces, conductively and radiatively decoupled from the spacecraft. Conductive decoupling is achieved by use of low-conductivity Titanium for the kinematic mounts, and the natural isolation required by the quasi-kinematic mount design. The radiative isolation is achieved by the application of a low-emissivity aluminized coating to the external of the SOU structure.

The thermal design utilizes a synthetic quartz (Suprasil 300) primary mirror with a 10nm-thick B4C coating that reflects the EUV radiation of interest for science but transmits the solar visible and near-infrared with little absorption. Much of the high flux solar radiation entering through the aperture passes through the instrument and is then reflected to space by the heat rejection mirror (HRM) attached to the rear of the instrument. The HRM assembly is a CFRP structure mounted to the rear of the instrument that houses a highly reflective vacuum deposited silver fold mirror.

The majority of the solar radiation that is reflected within the SOU by the primary mirror is intercepted by three pre-slit heat rejection mirrors (mounted before the slit) and reflected to a single heat dump. The heat dump is connected directly to the spacecraft provided hot element (HE) interface. These mirrors are configured so that just the required science beam is passed through to the slit. Baffles also intercept solar radiation that either diverges as it comes into the instrument or is off-axis due to spacecraft pointing away from Sun centre.

The detector assembly (DA) is conductively and radiatively isolated from the instrument surroundings at the mounting interface (by PEEK standoffs at the interface) and by virtue of a low-emissivity finish on the DA exterior. Heat generated internally and the low levels of parasitic heat to the assembly are rejected to the spacecraft provided cold element (CE) interface. This allows the APS sensors within the detector assembly to be passively cooled then individually controlled by SEB powered PID closed loop control active heaters to a set-point of  $-20^\circ\text{C}$ .

The primary thermal design driver is to manage, at perihelion, the solar load incident through the  $52 \times 52 \text{ mm}$  aperture in the heatshield. Figure 3 illustrates a top level summary of the model predictions for the nominal perihelion hot analysis case. About 71% of the 31.8 W entering the SOU cavity is transmitted through the primary mirror and reflected directly to space by the HRM. The remaining 9.1 W is absorbed within the SOU structure. Of this, 2.4 W is directed to the heat

dump, where it is conducted to the spacecraft hot element interface. There is a further 8 W incident on the structure surrounding the instrument aperture; the selection of appropriate coatings ensures that only 0.6 W is absorbed. In the perihelion case the surrounding spacecraft temperature is specified as 50 °C. The instrument structure averages about 55 °C due to the addition of absorbed solar loads and internal dissipation. It is noted that the view of the HRM structure to deep space provides radiative cooling which mitigates to an extent the heating effect of the absorbed solar loads. About half of the internally absorbed solar load is at the primary mirror (at the coating and within the silica substrate). The primary mirror is therefore warmer than its surroundings, operating at about 70 °C.

8 W incident on aperture surround  
(0.6 W absorbed)

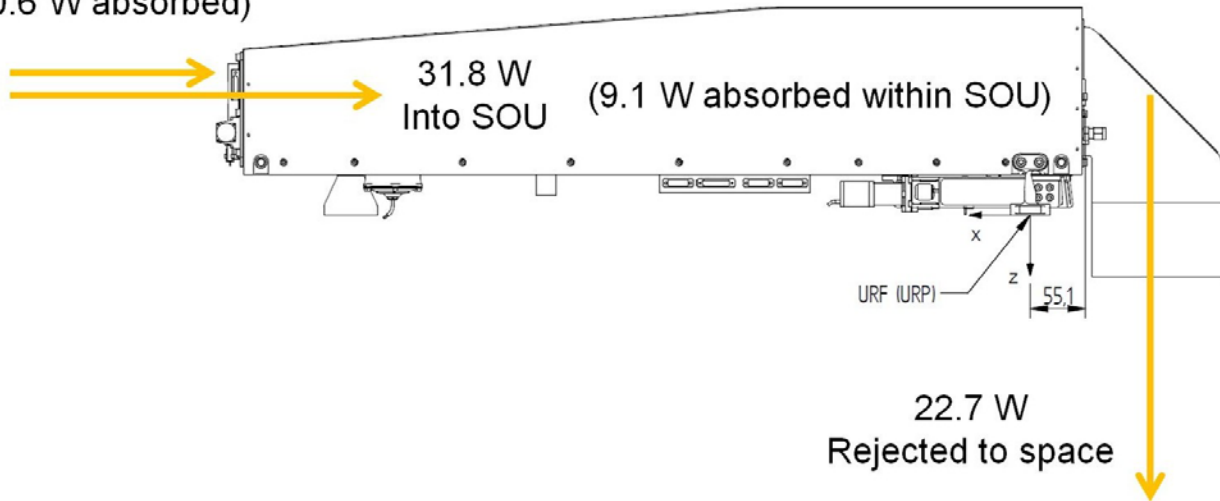


Figure 3. Thermal energy balance in the SPICE Optical Unit.

## 9. ACKNOWLEDGEMENTS

SPICE is an European-led instrument with contributions from the European Space Agency and the following ESA member states: France, Germany, Norway, Switzerland and the United Kingdom. This work has been funded by ESA, Centre National d'Etudes Spatiales (CNES), Deutsches Zentrum für Luft- und Raumfahrt (DLR), the Norwegian Space Centre, Swiss Space Office (PRODEX programme) and the UK Space Agency. The authors would like to thank the ESA Solar Orbiter Project Team and the industrial prime contractor Astrium UK for their support.

## REFERENCES

- [1] "Solar Orbiter: Definition Study Report", ESA/SRE 14 (2011)
- [2] Müller, D., Marsden, R. G., StCyr, O. G., Gilbert, H. R., "Solar Orbiter: Exploring the Sun–heliosphere connection". *Solar Phys.* 285, 25-70 (2013).
- [3] Kita, T., Harada, T., Nakano, N., Kuroda, H., "Mechanically ruled aberration-corrected concave gratings for a flat-field grazing-incidence spectrograph", *Appl. Opt.*, 22 (4) February 15, pp.512-513 (1983)
- [4] Harada, T., Sakuma, H., Ikawa, Y., Watanabe, T., Kita, T., "Design of high-resolution XUV imaging spectrometer using spherical varied line-space grating", *Proc. SPIE* 2517, 107-115 (1995).
- [5] Poletto, L. and Thomas, R.J., "Stigmatic spectrometers for extended sources: design with toroidal varied-line-space gratings", *Appl. Opt.* 43(10) Apr 1, 2029-38 (2004).